Optical recombination of biexcitons in semiconductors

M. Bauer,[1, *] J. Keeling,[2] M. M. Parish,[3, 1] P. López Ríos,[1] and P. B. Littlewood[1, 4]

[1]*Cavendish Laboratory, J J Thompson Avenue, Cambridge, CB3 0HE, United Kingdom*
[2]*Scottish Universities Physics Alliance, School of Physics and Astronomy,*
University of St Andrews, St Andrews KY16 9SS, United Kingdom
[3]*London Centre for Nanotechnology, Gordon Street, London, WC1H 0AH, United Kingdom*
[4]*Physical Sciences and Engineering, Argonne National Laboratory, Argonne, Illinois 60439, U. S. A.*

We calculate the photoluminescence spectrum and lifetime of a biexciton in a semiconductor using Fermi's golden rule. Our biexciton wavefunction is obtained using a Quantum Monte Carlo calculation. For a recombination process where one of the excitons within the biexciton annihilates, we find that the surviving exciton is most likely to populate the ground state. We also investigate how the confinement of excitons in a quantum dot would modify the lifetime in the limit of a large quantum dot where confinement principally affects the centre of mass wavefunction. The lifetimes we obtain are in reasonable agreement with experimental values. Our calculation can be used as a benchmark for comparison with approximate methods.

I. INTRODUCTION

Information about many-body systems of electrons and holes is primarily obtained through their luminescence. While good calculations on the ground states of these systems have been performed for a variety of electron and hole densities, good estimates of luminescence require the inclusion of final excited states, for which calculations are difficult. Thus, it is important to quantify how excited final states affect luminescence. In this paper, we solve essentially exactly the problem of decay of the simplest correlated system, namely the biexciton.

Luminescence of these biexcitons, which are bound states of excitons (electron-hole pairs), is potentially relevant for studying luminescence from semiconductor lasers. While semiconductor lasers correspond to the dense limit of the electron-hole phase diagram, where the electrons and holes ionise into a plasma[1], it is well known that the inclusion of correlation effects with the surrounding electrons and holes is necessary for a good estimate of semiconductor luminescence[2–4]. Moreover, a variational Monte Carlo study of the electron-hole phase diagram has revealed a surprisingly large excitonic insulator phase, which extends well into these high densities[5]. Thus, luminescence from excitonic states also contributes to light emission in the plasma. However, it is not a priori obvious whether emission from an independent exciton can adequately describe emission from a plasmonic state where interaction effects are crucial. This question of interaction can be addressed by considering the biexciton as the most complicated correlated state that can still be treated exactly. Since the detailed form of the bound state wavefunction can significantly affect the overlap with final states it is important to go beyond the use of simple analytical variational wavefunctions for the biexciton. Instead we use a biexcitonic wavefunction obtained from a quantum Monte Carlo calculation. Thus, our results can be used as a benchmark for larger and more complicated systems that currently still require approximate methods.

The concrete aim of this work is twofold: we primarily want to calculate the emission spectrum of the biexciton, using an essentially numerically exact biexciton wavefunction. We then want to find out how well the lifetime we calculate from this spectrum compares to experimental and other theoretical lifetimes.

For the calculation of the lifetime we focus on radiative recombination involving the emission of a photon. This process could potentially excite the surviving exciton into an excited state. In order to obtain both the emission spectrum and the lifetime we follow the procedure by Elliott[6] and use Fermi's golden rule, which requires the calculation of matrix elements between these exciton excited state and the full biexciton wavefunction. The wavefunctions and matrix elements are clearly different for different mass ratios. Hence, we consider different mass ratios where the hole mass m_h is equal to or much greater than the electron mass m_e for the spectra and several intermediate mass ratios for the calculation of the lifetime.

It has been shown in previous calculations[7] that the inclusion of the accurate semiconductor eigenstates, i.e. polariton states, is important for an accurate estimate of the biexciton lifetime. The importance of polariton effects for the biexciton decay comes from the fact that since most binding energies of excitonic molecules ε_m are much smaller than the polariton splitting parameter Ω_c, the dispersion of the final states after the decay process is strongly modified compared to the dispersion of the free exciton and photon states. Hence we estimate lifetime including polariton effects; in doing this we use insights from our calculation in the absence of polariton effects in order to simplify the calculation in presence of polaritons. We present a general formula of the typical non-radiative biexciton lifetime in the semiconductor, which should in principle work for materials where the polariton effect is weak.

To the extent that our Monte Carlo biexciton wavefunction is a good wavefunction, the remainder of our calculation is essentially exact for system where the polariton effect is negligible. We expect that shape of our emis-

sion spectra, calculated without polariton effects, will not be affected drastically even for materials where the effect is important. Thus, our calculation can be used as a comparator for approximate methods, which could, however, reach non-zero densities.

While our spectra are for 3D bulk only, we extend our lifetime calculation to a 3D quantum dot, since more experimental data is available there. We compare our lifetime estimates for a range of materials to experimental and other theoretical estimates. A similar procedure for the calculation of lifetimes as presented in this paper may also be applied to quantum well systems.

In this paper we calculate the simplest optical recombination process. The question of whether this is in fact responsible for the exciton lifetime is however more complicated as many other mechanisms can play a role. In semiconductor bulk systems these mechanisms for example include recombination involving impurities, or traps[8], or Auger recombination[9–15]. We discuss some of these later; however as our lifetimes compare reasonably with experimental values it seems that radiative recombination is the main channel for biexciton annihilation.

The paper is organised as follows: Section II discusses photoluminescence from biexcitons in a semiconductor, and section III discusses their lifetime. In section II A we introduce the approach used to determine the biexciton wavefunctions and how to calculate photoluminescence spectrum, which we present and discuss in section II B. Section III A presents the calculation of the biexcitonic lifetime with polariton effects and optionally confinement and section III B compares biexciton lifetimes for five semiconducting systems to experimental and some other theoretical values, and discusses their trends with electron/hole mass ratio and confinement. We conclude in section IV.

II. PHOTOLUMINESCENCE

A. Methods

In this section we present the calculation of luminescence from the biexciton. We first discuss the methodology of this calculation, starting from the light-matter interaction Hamiltonian, and the form of the biexcitonic wavefunction, before quoting the general formulae for the relative transition rates into different excited excitonic states. We then present the results and discuss our obtained emission spectra.

The light-matter interaction in second quantisation is given by

$$H' = \gamma \times \int dr \sum_{\sigma'=\pm} \sum_{\mathbf{k}_e, \mathbf{k}_h \in BZ} \frac{e}{m_0} \quad A_0$$
$$a^\dagger_{\mathbf{k}_e+\mathbf{k}_h, \sigma'} c^\dagger_{-\mathbf{k}_h, \sigma} c_{\mathbf{k}_e, -(\sigma-\sigma')} p_{cv} \quad (1)$$

where p_{cv} is the momentum matrix element for a transition of an electron with charge e and mass m_0

between the valence and the conduction band and $A_0 = \sqrt{\hbar/(2\epsilon\omega_k V)}$ is the standard vector potential field strength. This expression contains ω_k as the frequency of the emitted photon, the dielectric constant of the material ϵ, and a unit of box quantisation volume V which cancels in the latter part of the calculation. The operators $c^\dagger_{\mathbf{k}_{h/e}, \sigma}$ create holes and electrons with momentum k_h and k_e and with spin quantum number $\sigma = \pm\frac{3}{2}, \frac{1}{2}$, respectively. $a^\dagger_{\mathbf{k}, \sigma}$ creates a photon with polarisation $\sigma' = \pm 1$. p_{cv} is the optical or momentum matrix element between valence and conduction band. The factor γ in equation (1) accounts for the overlap of electron and hole spin states[16]; if spin-orbit coupling is neglected then this becomes simply a factor of two[17]. We use the values from Ref. 18.

The luminescence is determined by decay from all possible bound states in the semiconductors into other bound states through the emission of a photon. The rate of generating a photon per unit photon energy corresponds to the expectation value of the number of photons after a time t:

$$W(\hbar\omega) = \sum_{\mathbf{k}, \sigma} \frac{\langle a^\dagger_{\mathbf{k}, \sigma}(t) a_{\mathbf{k}, \sigma}(t) \rangle}{t} \delta(\hbar\omega - E(\hbar\omega, \sigma)), \quad (2)$$

where ω is the frequency corresponding the the emitted photon with wavevector $\mathbf{k}$, and $E(\hbar\omega, \sigma)$ is the dispersion of the photon in the medium. In this article, we consider luminescence from a biexciton in its ground state as a first approximation to understand luminescence from bound states in semiconductors; the result will hopefully allow us to estimate to what extent bound states will need to be considered, or whether the consideration of individual excitons suffices.

In order to obtain a more explicit equation for the luminescence than equation (2), we first of all need to discuss the wavefunction of our biexcitonic ground state with respect to which the expectation value of equation (2) is calculated. Previous calculations of luminescence from biexcitons have used estimates or simplified versions for the biexciton wavefunction[7]; In contrast, the biexciton wave function Ψ_{BE} we use is of the form

$$\Psi_{BE}(\mathbf{R}) = \exp[J(\mathbf{R})] \Psi_S(\mathbf{R}), \quad (3)$$

where $J(\mathbf{R})$ is a Jastrow factor of the Drummond-Towler-Needs form[19] containing only two-particle correlations, and

$$\Psi_S(\mathbf{R}) = \phi_1(r_{13})\phi_1(r_{24})\phi_2(r_{14})\phi_2(r_{23})$$
$$+ \phi_2(r_{13})\phi_2(r_{24})\phi_1(r_{14})\phi_1(r_{23}),$$

where r_{ij} is the distance between particles i and j, with electrons being particles 1 and 2, and holes being particles 3 and 4. The pairing orbitals $\phi_n(r)$ are of the form

$$\phi_n(r) = \exp\left[\frac{-r^2}{p_{1,n}(p_{2,n}+r)} + \frac{\Gamma p_{2,n} r}{p_{2,n}+r}\right], \quad (4)$$

where $p_{1,n}$ and $p_{2,n}$ are optimisable parameters and Γ is a constant such that the Kato cusp conditions[20] at electron-hole coalescence points is reproduced by Ψ_S; electron-electron and hole-hole cusps are introduced via the Jastrow factor.

Given a trial wave function Ψ, assumed to be real for simplicity, the variational Monte Carlo (VMC) method is capable of evaluating the variational estimate E_Ψ of the ground-state energy E_0,

$$E_\Psi = \frac{\int \Psi(\mathbf{R})\hat{H}(\mathbf{R})\Psi(\mathbf{R})d\mathbf{R}}{\int |\Psi(\mathbf{R})|^2 \, d\mathbf{R}} \geq E_0 \ , \qquad (5)$$

by evaluating the local energy,

$$E_L(\mathbf{R}) = \frac{\hat{H}(\mathbf{R})\Psi(\mathbf{R})}{\Psi(\mathbf{R})} \ , \qquad (6)$$

at a set of M configurations $\{\mathbf{R}_i\}$ distributed according to the square of the trial wave function $|\Psi(\mathbf{R})|^2$, and evaluating the average

$$E_\Psi \approx E_V = \frac{1}{M}\sum_{i=1}^{M} E_L(\mathbf{R}_i) \ , \qquad (7)$$

where the "approximately equal" sign refers to the statistical error due to the finite size of the sample. In addition, the VMC method optimises the parameters in the trial wave function by means of minimizing E_V with respect to the parameters, using techniques such as the modified linear least-squares method developed by Umrigar[21].

The above trial wave function is then optimised within VMC for different mass ratios using the CASINO code[22]. The VMC energies are presented in Table I, where we also report the variance of the local energies σ_V^2, which is an additional measure of the quality of a wave function. The variational energies obtained at all mass ratios contain a large fraction of the exact binding energy, indicating an accurate description of these systems. A comparison of VMC wavefunctions with both experimental and theoretical values was performed in[23] for quantum well structures.

m_h/m_e	E_V	σ_V^2
1837.36222	-1.1502(4)	0.131(1)
183.73622	-1.1335(2)	0.01831(5)
18.37362	-1.0338(1)	0.01587(5)
1.83736	-0.66725(8)	0.00511(2)

TABLE I. VMC energies and variances of the local energy for different hole-to-electron mass ratios.

Using the biexcitonic wavefunction calculation with VMC as our ground state, we can now transform equation (2) into Fermi's golden rule for the transition rate $W(\hbar\omega)$ per energy range of a particular photon[24]. Fermi's golden rule corresponds to a perturbative treatment of the interaction[25], and has already been used by Elliot[6] for a calculation of exciton luminescence. The transition rate per energy range requires a sum over all final states of both exciton and photon,

$$W(\hbar\omega) = \frac{2\pi}{\hbar}\sum_{\mathbf{k},\mathbf{K},\{n_i\}} |\langle \Psi_{E,\{n_i\},\mathbf{K}}|H'|\Psi_{BE}\rangle|^2 \qquad (8)$$
$$\delta(\epsilon_i - \epsilon_f(\mathbf{k},\{n_i\}) - \hbar\omega)\delta(\hbar\omega - \hbar c|\mathbf{k}|).$$

As final exciton momenta $\mathbf{K}$ are constrained by momentum conservation, the corresponding sum disappears, and the momentum of the surviving exciton is $-\mathbf{k}$. The final excitonic state with wavefunction $\Psi_{E,\{n_i\},\mathbf{K}}$ is labelled by the centre of mass $\mathbf{K}$ and the various eigenstates of the exciton $\{n_i\}$, which are standard hydrogenic solutions. The quantum numbers $\{n_i\}$ correspond to n, l, and m for the bound and k, l, and m for the continuum states. As the biexciton is in its ground state, we obtain from angular momentum conservation that $l = m = 0$ for the surviving exciton. ϵ_i is the ground state biexciton energy, and $\epsilon_f(\mathbf{k},n)$ the energy of the final state.

We now insert H' from equation (1) into equation (8) and notice that it is necessary to perform several real space integrals in order to simplify the matrix element. After a separation of centre of mass and relative coordinates, the relative exciton wavefunction $\phi_{E,n}$ can be expressed in terms of a single coordinate $\mathbf{r}_1 = \mathbf{r}_{e1} - \mathbf{r}_{h1}$, where $\mathbf{r}_{e1}$ and $\mathbf{r}_{h1}$ refer to the coordinates of electron and hole of the surviving exciton. The relative biexciton wavefunction ϕ_{BE} depends on this coordinate $\mathbf{r}_1$, and the coordinates of the second electron and hole, $\mathbf{r}_{e2}$ and $\mathbf{r}_{h2}$. In our relative coordinate system these are represented by a vector to their centre of mass, $\mathbf{r}_2 = (\mathbf{r}_{e1} + \mathbf{r}_{h1} - (\mathbf{r}_{e2} + \mathbf{r}_{h2}))/2$, and a relative coordinate $\mathbf{r}_3 = \mathbf{r}_{e2} - \mathbf{r}_{h2}$. The application of the dipole approximation, $\mathbf{p}_{op} \approx 0$ requires the annihilating electron and hole to be at the same point in space. Thus, this relative coordinate is zero, and so ϕ_{BE} has the functional dependence $\phi_{BE}(\mathbf{r}_1, \mathbf{r}_2, \mathbf{0})$. For the bulk system, the centre of mass coordinates can be integrated over analytically. We then obtain a formula for the transition rates R into the bound states n,

$$R_n = \frac{p_{cv}^2 e^2}{m_0^2}\frac{\sqrt{\varepsilon}}{2\varepsilon_0\pi}\frac{\omega_n}{\hbar c^3} \qquad (9)$$
$$2\left(\int d\mathbf{r}_1 d\mathbf{r}_2 \phi_{E,n}(\mathbf{r}_1)^* \phi_{BE}(\mathbf{r}_1, \mathbf{r}_2, \mathbf{0})f(\mathbf{r}_1, \mathbf{r}_2)\right)^2.$$

where we have introduced the function $f(\mathbf{r}_1, \mathbf{r}_2)$ to model confinement in a quantum dot. We will discuss this function in section III; for bulk, $f(\mathbf{r}_1, \mathbf{r}_2) = 1$. The additional factor of 2 in equation (9) comes from the fact that both excitons in the biexciton can recombine.

The frequency ω_n in equation (9) is the frequency associated with a specific transition. We neglect its momentum-dependence: The frequencies that contribute most to the emission spectrum will be close to the gap energy E_g and hence we approximate $\omega_n \to E_g/\hbar$ from here onwards. Our results confirm later that this treatment is
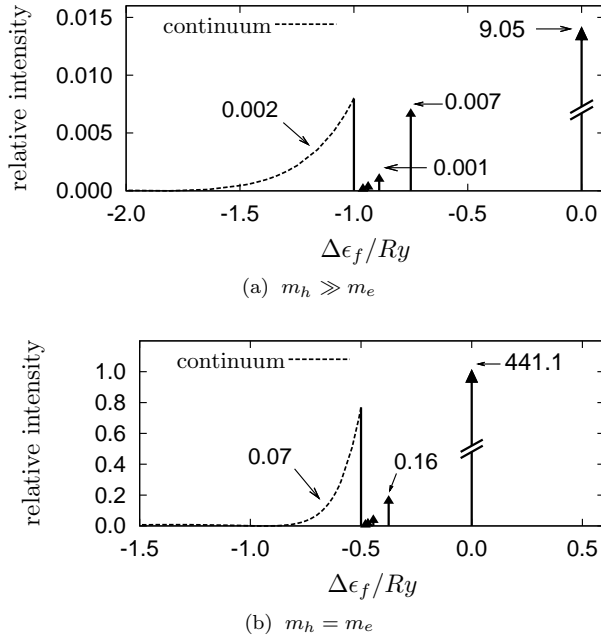
(a) $m_h \gg m_e$

(b) $m_h = m_e$

FIG. 1. Bulk emission spectra (overlap element as shown in Table II versus the energy difference of the surviving exciton with respect to its ground state, $\Delta\epsilon_f$) for the two limiting mass ratios. The emitted photon energy corresponds to $\hbar\omega = E_g - B_{2X} - 1Ry + \Delta\epsilon$ for $m_h \gg m_e$ and $\hbar\omega = E_g - B_{2X} - 0.5Ry + \Delta\epsilon$ for $m_h = m_e$, where B_{2X} is the biexciton binding and a single exciton has energy $E_g - 1Ry$ and $E_g - 0.5Ry$ for these two mass ratios, respectively. Note that the peaks from the discrete bound states are delta functions and hence represented by arrows, labelled by their intensity. While it is clear that the continuous part of the spectrum decays to zero for large energies E, there is a possibility for a small but finite overlap for intermediate E. The number labelling the continuum is its integrated weight.

indeed adequate. Thus the rate $R_n(n)$ in equation (9) is a function of quantum number n only.

Since R_n is the transition rate into a particular bound state, R_n and $W(\hbar\omega)$ are related by

$$W(\hbar\omega) = \sum_n R_n \delta(\hbar\omega - \hbar\omega_n) + W_{\text{continuum}}(\hbar\omega), \quad (10)$$

where $W_{\text{continuum}}(\hbar\omega)$ describes emission into continuum states. $W_{\text{continuum}}(\hbar\omega)$ can be obtained analagously to equation (9), with the only difference that the sum over discrete quantum numbers n in equation (8) becomes an integral over the continuum states and the continuum exciton eigenfunctions are confluent hypergeometric functions.

B. Results

The emission spectra from bulk for the two limiting mass ratios, $m_h = 1837m_e$ (corresponding to hydrogen), and $m_e = m_h$ are shown in Figure 1. As we have not

TABLE II. Dimensionless overlap elements, $2\int d\mathbf{r}_1 d\mathbf{r}_2 \phi_{E,n}(\mathbf{r}_1)^* \phi_{BE}(\mathbf{r}_1, \mathbf{r}_2, \mathbf{0})$, of excitonic bound (quantum number n) and continuum states with the biexciton wavefunction for various mass ratios. The mass ratios (m_h:m_e) correspond to decreasing the m_h from $1837m_e$ (in hydrogen) by factors of 10. Individual elements are converged to approximately %0.5 accuracy. An estimate of the absolute accuracy including the uncertainty of the wavefunction cannot be given, but we tentatively estimate 10% accuracy from comparisons with a different variational form. 'Total' indicates the sum over the calculated bound and continuum states, and the result from equation (12) is shown in the last row. We note that for $n \geq 2$ the values drastically decrease compared to $n = 1$ (base change as shown in the first column); however, these higher n matrix elements depend very sensitively on the form of the wavefunction.

m_h	1837	183.7	18.3	1.8	1.0
$n = 1$	9.1	20.4	79.6	427.0	441.1
$n = 2$ ($/10^{-3}$)	6.6	8.0	0.1	305.2	161.5
$n = 3$ ($/10^{-3}$)	1.0	1.0	0.4	18.3	34.8
$n = 4$ ($/10^{-3}$)	0.3	0.3	0.2	4.8	13.9
$n = 5$ ($/10^{-3}$)	0.2	0.1	0.1	4.1	6.8
bound total	9.1	20.4	79.6	427.3	441.3
continuum ($/10^{-2}$)	0.3	0.4	1.0	5.4	7.3
total	9.1	20.4	79.6	427.3	441.4
Equation (12)	9.1	20.4	79.6	427.4	441.5

included broadening, the delta-function peaks for transitions into the bound states are indicated by arrows, and labelled with the corresponding delta-function coefficient. Figure 1 shows clearly that the transition into the ground state dominates. The spectra for the intermediate mass ratios show a similar behaviour.

Individual overlap integrals for all different mass ratios are shown in Table II, which also contains the results obtained from equation (12). The discrepancy between the results from the individual overlaps ('total') and from equation (12) is a rough estimate of the numerical errors of the calculation. The agreement of these values shows that the results for the ground state are numerically stable. Further error associated with the results are due to the approximate shape and the parameters involved in the wavefunction. A different variational form for hydrogen gave bound state transition rates within 10% and continuum transition rates within about 30% of those in Table II. While one can tell that the overlaps with the higher excited states decrease with n, the actual individual numbers depend very sensitively on detailed properties of the numerically determined wavefunction and hence should not be interpreted too closely.

The general shape of the continuous part of our emission spectrum should nevertheless be correct. The shape is notably different to the shape of the single exciton absorption spectrum calculated by Elliott[6]. This single exciton absorption spectrum should correspond to a single

exciton emission spectrum, provided the single exciton emission is possibe: a single exciton in free space cannot recombine due to momentum conservation, but recombination is possible when impurities are present and momentum conservation is relaxed. Nevertheless, the continuum part of the single exciton and biexciton emission spectra are different. Similar to single exciton absorption, the biexciton continuum has a finite onset, but falls off rapidly with E, while the exciton absorption continuum line increases square-root-like for large energies. We expect the general trend of our spectrum to be correct, although we note that our continuum curve at energies of order $E \approx 1 Ry$ is numerically sensitive to details of the Monte Carlo wavefunction. In this energy range we sometimes obtain a small but finite overlap, which is due to the numerical integration being very sensitive to the variational form of the wavefunction in this energy range.

The continuum emission decreases with E due to the decreasing wavefunction overlap of the initial state with the higher energy exciton state after photon emission. The fast decrease of the continuum emission in Figure 1 is especially notable for equal masses. Such a biexciton involving particles with equal masses is more loosely bound than one with a heavier hole. Loosely bound excitons have a smaller binding energy and thus less energy is available from the recombination. As the binding energy decreases the recoil momentum of the surviving exciton, $\mathbf{K} = -\mathbf{p}_{op}$, decreases towards zero, where recombination is prohibited by momentum conservation. The weaker fall-off of the continuum curve for the tighter bound biexciton suggests that non-radiative processes, where the surviving exciton absorbs all the energy available from the annihilation, are more likely for heavier holes. When non-radiative decay is the main recombination mechanism, exciton lifetimes are dependent on charge carrier density or temperature[9,11].

The most notable feature of our calculation is the predominance of the $1s$ peak. This predominance implies that the surviving exciton is not affected by the recombination of the other-electron hole pair, even though we initially assume a strongly interacting bound state. Our model thus justifies treating excitons as non-interacting for the purpose of optical recombination. However, we speculate that interactions become more important if higher excited initial states are present.

The lineshapes in emission spectra from biexcitons are often broadened due to scattering with phonons[26,27]. This broadening smears out the different peaks from a variety of possible final states, and hence no direct comparison with our spectra is possible. Similar problems prevent measurements of lifetimes in bulk[28]. In addition, higher excited initial biexciton states may be present. However, our tentative spectra for bulk can be used as a reference point for other systems.

III. LIFETIMES

We now turn to the calculation of the biexcitonic lifetimes. We first discuss how to include polariton effects and present a general formula for the biexcitonic lifetime before turning to a brief discussion of lifetimes for a confined quantum dot. The results are also divided into a section on bulk and quantum dot systems. We compare to experimental and theoretical values in each of these subsections.

A. Methods

The overall rate for biexciton decay, which corresponds to the inverse biexcitonic lifetime, is made up from the individual transition rates in equation (10),

$$\frac{1}{T} = \int d(\hbar\omega) W(\hbar\omega)$$
$$= \sum_n R_n + \int d(\hbar\omega) W_{\text{continuum}}(\hbar\omega). \quad (11)$$

We note that the sum over excitonic states in equation (11) is complete and hence can be understood as a resolution of identity, and thus total biexciton decay rate can also be expressed in terms of the biexciton wavefunction only,

$$\frac{1}{T} = \frac{p_{cv}^2 e^2}{m_0^2} \frac{\sqrt{\varepsilon}}{2\varepsilon_0\pi} \frac{E_g}{\hbar^2 c^3}$$
$$2 \int d\mathbf{r}_2' d\mathbf{r}_1 d\mathbf{r}_2 \phi_{\text{BE}}(\mathbf{r}_1, \mathbf{r}_2, \mathbf{0}) \phi_{\text{BE}}(\mathbf{r}_1, \mathbf{r}_2', \mathbf{0}). \quad (12)$$

This expression should provide a check for the numerical errors associated with the integral.

The photon generation rate in equation (2) does not yet include the polaritonic eigenstates. We mention earlier that these are important for nearly all semiconductors, since the biexciton binding energy $\varepsilon_m \ll \Omega_c$ (the polariton splitting parameter) in almost all materials. The exact calculation of lifetime from a semiconductor would thus require the rate of polariton generation per unit energy

$$W(\hbar\omega) = \frac{1}{2} \sum_{\mathbf{k},s,\sigma} \frac{\langle \xi_{\mathbf{k},s,\sigma}^\dagger(t) \xi_{\mathbf{k},s,\sigma}(t) \rangle}{t}$$
$$\delta(\hbar\omega - E_{\text{polariton}}(\mathbf{k}, s, \sigma)), \quad (13)$$

where $\xi_{\mathbf{k},s,\sigma}^\dagger(t)$ creates a polariton with momentum $\mathbf{k}$ and spin σ in state s and $E_{\text{polariton}}$ is the corresponding dispersion. The factor of one half avoids double-counting, since in the biexciton decay two polaritons are generated.[29] In general the photon can be reabsorbed to form another biexciton and reemitted in many cycles. This would require a self-consistent treatment such as performed in Ref. 7, which we expect to be important

for materials with large Ω_c/ε_m. As we saw previously that the decay rate is dominated by the decay rate into the 1s exciton, we assume that the created polariton is a superposition of a 1s exciton and a photon and do not consider excited exciton states. We also use the resonant approximation for the polaritonic eigenstates, which we expect to cause an error of no more than 15%. With these approximations, our expression for the inverse lifetime becomes

$$\frac{1}{T} = \frac{\gamma}{2} \times |\langle \Psi_{\mathrm{E},\{n_i\},\mathbf{K}} | \Psi_{\mathrm{BE}} \rangle|^2 \times \Big\{ 2(E_0 - 2E_g)^2 +$$
$$\frac{[E_0(-E_0 + 2E_g) + \Omega_c^2]^2 \Omega_c^2}{2(E_0 - 2E_g)^2[(E_0 - 2E_g)^2 + \Omega_c^2]} \Big\}$$
$$\times \frac{p_{cv}^2 e^2}{m_0^2} \frac{\sqrt{\varepsilon^3}}{\pi\varepsilon\varepsilon_0 E_g/\hbar} \frac{1}{(\hbar c)^3}. \qquad (14)$$

Because lifetimes are longer and hence more extensively studied for confined systems, we wish to study the effect of confinement on the recombinative lifetime, and we consider a 3D quantum dot system. We assume a spherical quantum dot of radius d, where the photon wavelength $\lambda \gg d \gg a_E, a_B$, where a_E and a_B are relevant exciton and biexciton lengthscales. The exciton lengthscale a_E is the distance between the electron and hole in the surviving exciton, and the biexciton lengthscale a_B is the distance between the centres of mass of the two excitons in the biexciton. Such a dot is large enough to only affect the centre of mass, but not the relative wavefunction. The centre of mass wavefunctions can then be expressed in terms of spherical Bessel functions, and we obtain the constraint that the centre of mass wavefunction of the surviving exciton must also be in the ground state. Again, we use the 1s exciton-polariton wavefunction; the corresponding lifetime is $R(n = 1)$ in equation (9). The effect of confinement is reflected in the function $f(\mathbf{r}_1, \mathbf{r}_2)$ in equation (9), where

$$f(\mathbf{r}_1, \mathbf{r}_2) = \frac{4d}{\pi} \frac{\sin(\frac{\pi}{d} \frac{|\mathbf{r}_2|}{2})}{|\mathbf{r}_2|}.$$

B. Results

We have calculated lifetime estimates for a number of materials, and compare these to experimental and other theoretical lifetime estimates in this section. The parameters required for the calculations of these lifetimes for CuCl, GaAs, ZnSe and InGaAs are given in table III, and table IV contains quantum dot values for those parameters which differ between bulk and quantum dot systems. Since the calculated lifetimes depend quite sensitively on the correct parameter and there is some variation of parameters in the literature, this comparison is quite difficult. One example is e.g. the InGaAs mass ratio, where different groups use bulk or quantum well or interpolated quantum well mass ratios, or the experimental GaAs lifetime. Here we quote an experimental value

for GaAs bulk lifetime of 1.8 ns in table V merely for completeness, since we expect the real lifetime to be around 10-100 ps[30]. This estimate is based on the fact that the bulk biexciton lifetime should be smaller than the lifetime in confined system like quantum dots or quantum wells, where the biexciton binding energy is higher[31]. For quantum wells, the biexcitonic lifetime is expected to be around half the excitonic lifetime[32,33], which in Ref. 33 is quoted to be of order 200 ps, while Ref. 34 contains an estimate of 10 ps for the excitonic lifetime and Ivanov et al. 7. quote lifetimes of order of magnitude 1-10 ps. There exists nevertheless a higher lifetime estimate of 1 ns[35] for quantum dots; however Ref 34 cite potential impurities as a reason for lifetimes of this order of magnitude in quantum wells. Thus, the variety in experimental values makes the comparison sometimes somewhat difficult.

1. Bulk

We now discuss polariton lifetimes for bulk materials and the variation of the lifetime with mass ratio.

Without including polariton effects the lifetime for CuCl according to equation 14 would be 20 and 100 ps for mass ratios 1.8 and 18, respectively. The experimental lifetimes are between 18 and 24 ps[38,39] for a mass ratio $m_h/m_e \approx 5$, which shows that the inclusion of polaritonic states (giving instead lifetimes 9 ps and 47 ps for the same mass ratios) is indeed crucial. For the three semiconductors GaAs, ZnSe and CuCl experimental and our calculated lifetimes are shown in table V. We expect our method to work well for small ratios Ω_c/ε_m, while for large Ω_c/ε_m a full bipolariton wavefunction and thus the inclusion of recursive exciton creation and annihilation processes is necessary. Additional errors in our estimate are associated with intrinsic errors of the wavefunction, the numerical integration, the uncertainty of the material parameters, the different geometry of the quantum dot and the fact that experimentally, the exciton might leak out.

Indeed, our lifetime estimates for CuCl between 9 and 47 ps for mass ratios 1.8 and 18, respectively, agree reasonably with the experimental value for the intermediate mass ratio of $m_h/m_e \approx 5$. Ivanov et. al.[7] also obtain excellent agreement when using the bipolariton wavefunction, but quote a poor lifetime estimate when using the giant oscillator model[63] (4 ps). The improved wavefunction and a different weight in front of the process responsible for creating two lower state polaritons in equation 14 account for this difference.

For ZnSe and GaAs the increased ratio Ω_c/ε_m indicates that polariton effects should matter more. Indeed, our lifetime estimates are lower than the experimental values by about factor of 10.

Figure 2 shows plots of the dependence of the lifetime on mass ratio, with parameters for CuCl. The decrease of lifetimes on approaching the equal mass ratio limit in Figure 2(a) is initially counterintuitive as electron and

TABLE III. Semiconductor parameters with references. ε_m is the biexciton binding energy.

constant	GaAs	ZnSe	CuCl	In$_{0.6}$Ga$_{0.4}$ As
ε_m/meV	0.13[44], 0.45[45], 0.7± 0.2[36]	3.5[46]	32[47], 34[7], 42[48], 42[49]	2[42]
E_g	1.5[24]	2.8[50]	3.2[7]	0.7[50]
ε	13.1[24]	8.1[50]	5.6[7], 5.0[51]	14.3[52], 14.03[53]
m_h/m_0	0.5[24]	1.7[50]	1.8[47], 2.0[51]	0.46[54]
m_e/m_0	0.067[24]	0.017[50]	0.5[47,51]	0.04[53], 0.05[55], 0.067[43] a
Ω_c/meV	15.6[7]	100[50]	191[7]	7
E_p b	25.7[24]	29.56 (from[57])	2.3	21.7[53]

a from bulk values, but inclusion of strain effects in Hamiltonian

b E_p and Ω_c are related via the formula $\Omega_c = 2\sqrt{\gamma}\sqrt{2\pi}p_{cv}\hbar/(m_0\sqrt{4\pi\epsilon\omega_0\hbar}\sqrt{\pi a_E^3})$ and thus one can be derived from the other. The value of E_p in InGaAs where we do not quote a source was generated by this formula; note that the Ω_c of $100\mu eV$ measured by[56] is for a quantum dot in a nanocavity and thus not immediately applicable. For all other materials E_p is taken from the quoted source.

TABLE IV. Quantum parameters with references. ε_m is the biexciton binding energy.

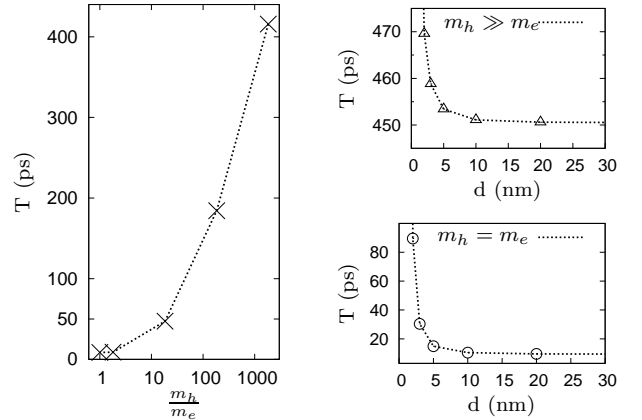| constant	CuCl	In$_{0.6}$Ga$_{0.4}$ As
ε_m/meV	50[58] (3nm), 51[49], 60[59] (3nm)	2[42]
m_h/m_0	1.8 a	0.125[60]b, 0.2[55], 0.46a, 0.5[43] c

a from bulk

b from interpolation between InAs and GaAs masses, using quantum well masses from[61] and[62]

c from bulk values, but inclusion of strain effects in Hamiltonian

TABLE V. Lifetime estimates for several semiconducting materials and experimental values for comparison. τ_{theor} corresponds to other theoretical calculations of biexciton lifetimes that are discussed in the text.. We expect the correct lifetime for GaAs to be of order 10-100 ps (see main text for discussion).

	bulk			quantum dot	
	GaAs	ZnSe	CuCl	CuCl	In$_{0.6}$Ga$_{0.4}$ As
τ/ps	0.5 -2.7	0.4 - 2.0	8.8-47.3	47.4-66.9	5.5-12.8
$\tau_{\exp}/ps$	1800[36]	40[37]	18-27[38,39]	65[40]	500[41]
τ_{theor}/ps	-	-	24[7]	-	500[42,43]

(a) Lifetime versus mass ratio on logscale

(b) Lifetime versus dot size

FIG. 2. Left panel: Biexciton lifetimes (in ns) in 3D bulk, calculated with approximate values for a CuCl semiconductor, for different mass ratios as shown in Table II. Right panel: Biexciton lifetime for hole masses $m_h = 1837m_e$ and $m_h = m_e$ for different CuCl quantum dot radii.

hole are much more likely to be at the same place for annihilation in the more tightly bound hydrogenic exciton. We find however that the probability for recombination is highest when the two excitons within the biexciton are far apart. This dependence on the mass ratio can be explained by the relative importance of the biexciton lengthscale a_B (the distance between the centre of masses of the two excitons) and the exciton lengthscale a_E (the distance between electron and hole within an exciton) in the overlap integral in equation (9).[64] The reason for the influence of the distance a_B on the recombination rate comes from the overlap integral in equation (9): the single exciton final state is delocalised. The overlap with the biexciton wavefunction is thus higher for a biexciton wavefunction in which the centres of mass of the excitons are more delocalised, i.e. where a_B is large. The lengthscale ratio a_B/a_E is inversely proportional to the ratio of biexcitonic to excitonic binding energies, and the

latter decreases towards the equal mass ratio limit for both two and three dimensional systems[65,66]; thus, in the equal mass biexciton, the excitons are loosely bound and are further apart.

2. Quantum dot

We now turn to lifetimes of confined systems, and discuss both the impact of confinement on the lifetime as well as some calculated lifetimes for two materials.

Figure 2(b) shows the effect of confinement in a spherical quantum dot where confinement principally affects the centre of mass wavefunction. Stronger confinement increases the exciton localisation and thus the increase of lifetime with confinement shown in Figure 2(b) is consistent with the previous argument of increased annihilation probability for biexcitons made up of a loosely bound exciton pair.

Unfortunately, experiments are not typically in the regime where confinement principally affects the centre of mass wavefunction, and so accurate numerical predictions of the biexciton lifetimes in these cases require specific calculations for the particular structures. Such specific calculations have for example been performed for $In_{0.6}Ga_{0.4}As$ quantum dots. Using a configuration interaction method, Narvaez et al. [42] obtain the exact experimental value of 0.5 ns for a $252 \times 252 \times 75$ Å $In_{0.6}Ga_{0.4}As$ quantum dot, which agrees well with the experimental lifetime of 0.5 ns of a dot with height 20Å and a square base with length 150-200Å[41]. Wimmer et al. [43] perform a Monte Carlo optimisation of wavefunctions in anisotropic quantum dots for three materials, among them $In_{0.6}Ga_{0.4}As$, and obtain excellent lifetime estimates for all three materials. Since the exciton Bohr radius for this system is about 200Å and the wavefunction is thus strongly affected by confinement effects, our wavefunction is a inaccurate estimate for this system. Additionally, our calculation does not take into account strain effects and anisotropy of the hole masses, which are nonnegligible effects for InGaAs. For example, it is well known that these effects have a large impact on gyromagnetic ratio[67], where realistic k.p simulations specific to the material provide estimates adequate to the experimental data[68]. Neglecting these effects and approximating this quantum dot by a spherical quantum dot of radius 100Å, we obtain a lifetime estimate of 6-13 ps, which is clearly inaccurate.

For 3 nm CuCl quantum dots, the quantum dot radius is larger than the excitonic Bohr radius of 6.8Å and thus our wavefunction should still be viable. Here, obtain a biexciton lifetime estimate of 47 -67 ps for our two limiting mass ratios, which is comparable to the experimental value of 65 ps. This shows that our method is indeed reasonable for the systems with small polariton effects, and can provide good estimates of the lifetime.

IV. CONCLUSIONS

In this article we have investigated the lifetime and emission spectrum of a biexcitonic system in different mass limits. We employ the approach by Elliott in order to find the transition rates into excitonic states using Fermi's golden rule. We find that in our model, which assumes an initial biexciton in the ground state, the annihilation of one electron and hole is most likely to result in an exciton in its ground state. The predominance of this transition means that the two excitons which form the excitonic molecule can be treated as non-interacting for the purpose of optical recombination. Our estimates of lifetimes for different mass ratios are comparable to experimental values.

In this calculation we have assumed a biexciton which was initially in its ground state. The presence of higher excited states could lead to a stronger overlap with higher excited final states, and thus to shorter lifetimes. We have also neglected the possibility of collision with other particles which could also lead to shorter lifetimes. We find that the biexciton lifetime slightly increases in confined quantum dots. Using an appropriately generated wavefunction, our method is also applicable for smaller quantum dots or quantum wells.

Interesting extensions to fully model quantum dots could include strain effects and for example the impact of the wetting layer, for which experimental data is also available[69]. It would also be interesting to calculate lifetimes for pumped systems, where the timescale of the biexciton lifetimes is important for an accurate estimation of the efficiency of multi-exciton generation[70,71].

Our approach can be used as a benchmark for comparing approximative methods for systems at finites densities. We also hope that the relative simplicity of the biexciton emission spectrum as found here may imply that the development of further experimental and theoretical understanding of emission from the dense electron-hole plasma is within reach.

* msb50@cam.ac.uk
1 P. B. Littlewood, G. J. Brown, P. R. Eastham, and M. H. Szymanska, Phys. Status Solidi B **234**, 36 (2002)
2 H. Haug and H. Haken, Z. Phys. A: Hadrons Nucl. **204**, 262 (1967)
3 H. Haug and S. W. Koch, *Quantum theory of the optical and electronic properties of semiconductors*, 5th ed. (World Scientific, Singapore, 2009)
4 S. Schmitt-Rink, C. Ell, and H. Haug, Phys. Rev. B **33**, 1183 (1986)

[5] X. Zhu, M. S. Hybertsen, and P. B. Littlewood, Phys. Rev. B **54**, 13575 (1996)

[6] R. J. Elliott, Phys. Rev. **108**, 1384 (1957)

[7] A. L. Ivanov, H. Haug, and L. V. Keldysh, Physics reports **296**, 237 (1998)

[8] W. Shockley and W. T. Read, Phys. Rev. **87**, 835 (1952)

[9] A. Haug, Solid-State Electron. **21**, 1281 (1978)

[10] L. Pincherle, Proc. Phys. Soc. London, Sect. B **68**, 319 (1955)

[11] A. R. Beattie and P. T. Landsberg, Proc. R. Soc. London Ser. A **249**, 16 (1959)

[12] Y. Liu and D. Snoke, Solid State Commun. **140**, 208 (2006)

[13] G. M. Kavoulakis, G. Baym, and J. P. Wolfe, Phys. Rev. B **53**, 7227 (1996)

[14] G. M. Kavoulakis and G. Baym, Phys. Rev. B **54**, 16625 (1996)

[15] A. Jolk, M. Jörger, and C. Klingshirn, Phys. Rev. B **65**, 245209 (2002)

[16] F. Bassani and G. Pastori Parravicini, *Electronic states and optical transitions in solids* (Pergamon, 1975)

[17] L. C. Andreani, in *Confined electrons and photons: new physics and applications*, edited by E. Burstein and C. Weisbuch (Plenum Publishing Corporation, 1995) p. 57

[18] L. C. Andreani and F. Bassani, Phys. Rev. B **41**, 7536 (1990)

[19] N. D. Drummond, M. D. Towler, and R. J. Needs, Phys. Rev. B **70**, 235119 (2004)

[20] T. Kato, Commun. Pure Appl. Math. **10**, 151 (1957)

[21] J. Toulouse and C. J. Umrigar, J. Chem. Phys. **126**, 084102 (2007)

[22] R. J. Needs, M. D. Towler, N. D. Drummond, and P. López Rí os, J. Phys.: Condens. Matter **22**, 023201 (2010)

[23] R. M. Lee, N. D. Drummond, and R. J. Needs, Phys. Rev. B **79**, 125308 (2009)

[24] S. L. Chuang, *Physics of optoelectronic devices* (Wiley New York, 1995)

[25] L. I. Schiff, *Quantum Mechanics* (Mc Graw-Hill Inc., 1968)

[26] H. Akiyama, T. Kuga, M. Matsuoka, and M. Kuwata-Gonokami, Phys. Rev. B **42**, 5621 (1990)

[27] M. Nagai and M. Kuwata-Gonokami, J. Lumin. **100**, 233 (2002)

[28] L. M. Herz and R. T. Phillips, Nat. Mater. **1**, 212 (2002)

[29] Equation (13) calculates the general decay rate into a two-polariton state and not the rate at which photons are emitted from the semiconductor, since it is this general decay rate that is experimentally accessible.

[30] J. J. Finley, Private Communication (2012)

[31] R. T. Phillips, D. J. Lovering, G. J. Denton, and G. W. Smith, Phys. Rev. B **45**, 4308 (1992)

[32] R. Spiegel, G. Bacher, A. Forchel, B. Jobst, D. Hommel, and G. Landwehr, Phys. Rev. B **55**, 9866 (1997)

[33] S. Charbonneau, T. Steiner, M. L. W. Thewalt, E. S. Koteles, J. Y. Chi, and B. Elman, Phys. Rev. B **38**, 3583 (1988)

[34] B. Deveaud, F. Clérot, N. Roy, K. Satzke, B. Sermage, and D. S. Katzer, Phys. Rev. Lett. **67**, 2355 (1991)

[35] R. Cingolani, K. Ploog, G. Peter, R. Hahn, E. O. Göbel, C. Moro, and A. Cingolani, Phys. Rev. B **41**, 3272 (1990)

[36] T. W. Steiner, A. G. Steele, S. Charbonneau, M. L. W. Thewalt, E. S. Koteles, and B. Elman, Solid State Commun. **69**, 1139 (1989)

[37] Y. Yamada, T. Mishina, Y. Masumoto, Y. Kawakami, S. Yamaguchi, K. Ichino, S. Fujita, S. Fujita, and T. Taguchi, Phys. Rev. B **51**, 2596 (1995)

[38] M. Hasuo, M. Nishino, and N. Nagasawa, J. Luminescence **60**, 672 (1994)

[39] A. L. Ivanov, M. Hasuo, N. Nagasawa, and H. Haug, Phys. Rev. B **52**, 11017 (1995)

[40] K. Edamatsu, J. Luminescence **70**, 377 (1996)

[41] S. M. Ulrich, M. Benyoucef, P. Michler, N. Baer, P. Gartner, F. Jahnke, M. Schwab, H. Kurtze, M. Bayer, S. Fafard, Z. Wasilewski, and A. Forchel, Phys. Rev. B **71**, 235328 (2005)

[42] G. A. Narvaez, G. Bester, and A. Zunger, Phys. Rev. B **72**, 245318 (2005)

[43] M. Wimmer, S. V. Nair, and J. Shumway, Phys. Rev. B **73**, 165305 (2006)

[44] A. Kuther, M. Bayer, A. Forchel, A. Gorbunov, V. B. Timofeev, F. Schäfer, and J. P. Reithmaier, Phys. Rev. B **58**, R7508 (1998)

[45] K. Kuroda, T. Kuroda, K. Sakoda, K. Watanabe, N. Koguchi, and G. Kido, Appl. Phys. Lett. **88**, 124101 (2006)

[46] Y. Yamada, T. Mishina, Y. Masumoto, Y. Kawakami, J. Suda, S. Fujita, and S. Fujita, Phys. Rev. B **52**, R2289 (1995)

[47] M. Ueta, H. Kanzaki, K. Kobayashi, Y. Toyozawa, and E. Hanamura, *Excitonic Processes in Solids*, Vol. 60 (Springer Series in Solid-State Sciences, 1986)

[48] T. Itoh, F. Jin, Y. Iwabuchi, and T. Ikehara, Springer Proceedings in Physics **36**, 76 (1989)

[49] S. Park, G. Jeen, H. Kim, and I. Kim, Journal of the Korean Physical Society **37**, 309 (2000)

[50] Y. Nozue, M. Itoh, and K. Cho, Journal of the Physical Society of Japan **50**, 889 (1981)

[51] L. C. Andreani, A. D'Andrea, and R. Del Sole, Phys. Lett. A **168**, 451 (1992)

[52] J. Singh, *Electronic and optoelectronic properties of semiconductor structures* (Cambridge University Press, 2003)

[53] O. Stier, M. Grundmann, and D. Bimberg, Phys. Rev. B **59**, 5688 (1999)

[54] S. Adachi, *Physical Properties of III-V Semiconductor Compounds* (Wiley Online Library, 1992)

[55] Y.-H. Liao, J. I. Climente, and S.-J. Cheng, Phys. Rev. B **83**, 165317 (2011)

[56] A. Laucht, N. Hauke, J. M. Villas-Bôas, F. Hofbauer, G. Böhm, M. Kaniber, and J. J. Finley, Phys. Rev. Lett. **103**, 087405 (2009)

[57] M. Willatzen, M. Cardona, and N. E. Christensen, Phys. Rev. B **51**, 17992 (1995)

[58] S. V. Nair and T. Takagahara, Phys. Rev. B **55**, 5153 (1997)

[59] Y. Masumoto, S. Okamoto, and S. Katayanagi, Phys. Rev. B **50**, 18658 (1994)

[60] D. V. Bulaev and D. Loss, Phys. Rev. Lett. **95**, 076805 (2005)

[61] K. S. Chan, Journal of Physics C: Solid State Physics **19**, L125 (1986)

[62] T. Wimbauer, K. Oettinger, A. L. Efros, B. K. Meyer, and H. Brugger, Phys. Rev. B **50**, 8889 (1994)

[63] E. Hanamura, Solid State Commun. **12**, 951 (1973)

[64] We note that the lengthscales a_B and a_E are only appropriate for describing this problem if the biexciton can be envisaged as being made up of two excitons that retain their identity in the bound state. This picture of a biexciton has been found to be correct at least in two dimensional systems with large electron-hole layer separation[23,72,73].

[65] L. Bányai, I. Galbraith, C. Ell, and H. Haug, Phys. Rev. B **36**, 6099 (1987)

[66] W. Xie, J. Phys.: Condens. Matter **13**, 3149 (2001)

[67] T. Nakaoka, T. Saito, J. Tatebayashi, and Y. Arakawa, Phys. Rev. B **70**, 235337 (2004)

[68] V. Jovanov, T. Eissfeller, S. Kapfinger, E. C. Clark, F. Klotz, M. Bichler, J. G. Keizer, P. M. Koenraad, G. Abstreiter, and J. J. Finley, Phys. Rev. B **83**, 161303 (2011)

[69] T. Kazimierczuk, A. Golnik, P. Kossacki, J. A. Gaj, Z. R. Wasilewski, and A. Babiński, Phys. Rev. B **84**, 115325 (2011)

[70] A. J. Nozik, Chem. Phys. Lett. **457**, 3 (2008)

[71] W. M. Witzel, A. Shabaev, C. S. Hellberg, V. L. Jacobs, and A. L. Efros, Phys. Rev. Lett. **105**, 137401 (2010)

[72] C. Schindler and R. Zimmermann, Phys. Rev. B **78**, 045313 (2008)

[73] A. D. Meyertholen and M. M. Fogler, Phys. Rev. B **78**, 235307 (2008)